The International Journal of Advanced Manufacturing Technology
January 2014, Volume 70, Issue 1-4, pp 523-530

External Grind Hardening Forces Modelling and Experimentation

K. Salonitis[1]*, P. Stavropoulos[2], A. Kolios[3]

(1) Cranfield University, Manufacturing and Materials Department, UK

(2) University of Patras, Lab. for Manufacturing Systems & Automation, Greece

(3) Cranfield University, Offshore, Process & Energy Engineering Department, UK

* k.salonitis@cranfield.ac.uk and salonitisk@gmail.com

P: +44(0)1234758347, F: +44(0)1234751172

Abstract

Grind hardening process utilizes the heat generated in the grinding area for the surface heat treatment of the workpiece. The workpiece surface is heated above the austenitizing temperature by using large values of depth of cut and low workpiece feed speeds. However, such process parameters combinations result in high process forces that inhibit the broad application of grind hardening to smaller grinding machines. In the present paper, modelling and predicting of the process forces as a function of the process parameters is presented. The theoretical predictions present good agreement with experimental results. The results of the study can be used for the prediction of the grind-hardening process forces and therefore, optimize the process parameters so as to be used with every size grinding machine.

Keywords

Grind-hardening, grinding forces, modelling

1 BACKGROUND

Grind-hardening is a special grinding process that can simultaneously harden and grind roughly a workpiece. The process is based on the utilization of the process generated heat for inducing a suitable temperature field on the workpiece, capable of producing high surface hardness. This is achieved as the dissipated heat and the subsequent quenching of the workpiece induce martensitic transformation to the workpiece surface.

The grind-hardening process is a relatively new one that was introduced by Brinksmeier and Brockhoff [1]. The main process parameters are the workpiece speed, the depth of cut, the cutting speed, the workpiece material and the grinding wheel type. Most of the published works have been concentrated on modelling the effect of these process parameters on Hardness Penetration Depth (HPD) and hardness distribution. Brockoff [2] and Brinksmeier *et al*. [3] presented experimental works whereas Chryssolouris *et al*. [4] and Salonitis *et al*. [5 - 7] dealt with the grind-hardening subject on a theoretical basis.

Few papers presented have focused on the prediction of the process forces induced by the grind-hardening process. Some first experimental trends where identified by Brockoff [2]. Chryssolouris *et al*. [4] for the prediction of the heat flux generated in the grinding zone, have estimated theoretically the grinding forces from the average contact pressure that grinding wheel exerts on the workpiece material.

Grind-hardening process present a lot of similarities with conventional grinding in terms of process mechanisms. A number of models have been presented for

estimating the grinding forces in a number of different grinding processes, such as conventional pendulum grinding, creep feed grinding and high efficiency deep grinding. Chang and Wang [8] considered the random nature of grit distribution as an important criterion. Durgumahanti et al. [9] modelled mathematically both tangential and normal components of chip formation force, sliding force and ploughing force and experimentally validated for conventional grinding process. One of the most most popular grinding forces model was developed for estimating the normal component of force by Werner [10] and was recently revisited by Mishra and Salonitis [11] for the case of creep feed grinding. One key finidng of the literature review is that almost all available grinding force models are empirical and rely on a big number of experimental data for estimating their coefficients. Furthermore, they relate grinding forces only to the process parameters and no model has been presented up to now able to take into consideration the characteristics and specifications of the grinding wheel.

The process forces are one of the most important parameters in evaluating the entire grinding process. The normal forces affect the surface deformation and roughness of the workpiece, while the tangential grinding forces influence the power consumption and service life of the grinding wheel. In the case of grind-hardening, these forces are quite higher than the ones measured during the conventional grinding process, inhibiting the broad application of grind-hardening to smaller grinding machines.

The scope of the present paper is to investigate the effect of the process parameters and the grinding wheel specifications (structure, hardness and grain size) on the induced process forces of grind-hardening.

2 THEORETICAL ANALYSIS

The theoretical estimation of grinding forces is based on authors' previously published study [7], and presented here in greater detail. The grinding forces can be analysed into a tangential (F_t) and a normal component (F_n). Alternatively grinding forces can be also described by their horizontal (F_h) and vertical (F_v) components as can be seen in Figure 1. Since the diameter of the grinding wheel is much larger than the depth of cut, the horizontal component can be assumed to be identical to the tangential one.

The common practice in papers found in the literature is to obtain the total grinding force by summing up the grinding force exerted by each individual grain in the grinding zone [12 – 15]. Alternatively, the total grinding force can be represented as the sum of the grinding force exerted for the chip formation, for the plastic deformation (plowing) of the workpiece and for the sliding of the grinding grains on the workpiece surface.

$$F_t = F_{t,sl} + F_{t,ch} + F_{t,pl} \quad (1)$$

where $F_{t,sl}$, $F_{t,ch}$ and $F_{t,pl}$ are the tangential force for sliding, for chip formation and for plowing respectively. The cutting forces include the forces exerted for chip formation and plowing:

$$F_c = F_{t,ch} + F_{t,pl} \quad (2)$$

2.1 Sliding forces

Malkin [16], based on experimental results, has correlated the sliding forces with the friction coefficient between the workpiece material and the grinding wheel, the average contact pressure and the area of contact:

$$F_{t,sl} = \mu \cdot p_m \cdot A_a \tag{3}$$

where μ is the friction coefficient between the workpiece material and the abrasive grains, p_m is the average contact pressure of the abrasive grains on the workpiece and A_a is the actual area of contact between the abrasive grains and the workpiece.

2.1.1 Average contact pressure

Malkin [16] has conducted a number of experiments with various grinding wheels and different process parameters and has proved that the average contact pressure depends solely on the cutting curvature difference. In the case of the grinding wheel speed u_s being significantly higher than the workpiece speed u_w, the average contact pressure can be estimated by [4]:

$$p_m = k_1 \frac{4u_w}{d_e u_s} + k_2 \tag{4}$$

where d_e is the equivalent diameter, and k_1 and k_2 are linear coefficients that are experimentally defined and can be considered to be a function of processing environment (grinding machine, coolant type etc.).

2.1.2 Actual area of contact

The actual area of contact between the grains and the workpiece depends on the process parameters and on the grinding wheel composition. The specification of a grinding wheel describes comprehensively its composition.

It is assumed that the heat is generated only between the grains and the workpiece material. Therefore, the actual area of contact is the product of the number of active grains n_a adjacent to the workpiece surface and the average wear flat area A_g per grain.

$$A_a = n_a \cdot A_g \tag{5}$$

The number of active grains can be determined as a fraction of the number of static grains in the grinding zone.

$$n_a = \Phi_a \cdot n \tag{6}$$

where Φ_a is the fraction of static grains that are active.

A simple estimation of the number of static grains intersected by the grinding arc area can be determined by considering a finite volume including all the grains in the contact area, as it can be seen in Figure 2. This finite volume will have its three dimensions equal to contact length, grinding wheel width and grain height. The grains are considered spherical, thus the height of each grain will be equal to the average grain diameter. The total number of static grains can be considered to be the maximum number of grains included in the finite volume, and can be estimated using the following equation:

$$n = 6 \cdot V_g \cdot \frac{l_c \cdot b}{\pi \cdot d_g^2} \quad (7)$$

Where V_g is the volumetric concentration of abrasive grains in the wheel, l_c is the geometric length of contact zone ($l_c=\sqrt{d_e a_e}$), d_e is the equivalent diameter, a_e is the depth of cut, b is the grinding wheel width and d_g is the average diameter of the grains.

The average grain diameter is correlated with the grain size number M from the grinding wheel marked with the following equation:

$$d_g = 15.2 \cdot M^{-1} \quad (8)$$

The above equation approximates the grit dimension d_g as 60% of the average spacing between adjacent wires in a sieve, whose mesh number equals the grit number M.

The volumetric concentration of the abrasive grains, the grain diameter and the porosity of the grinding wheel are characteristics defined while it is being manufactured and its specifications are depicted qualitatively in its specifications. Malkin [16] has expressed the volumetric concentration of abrasive grains as a function of the wheel structure number S:

$$V_g = \frac{2(32 - S)}{100} \quad (9)$$

The fraction of active grains depends on a number of factors, such as the elasticity and the deformation of the grinding wheel, as well as of the workpiece during the grinding process, etc. For the needs of the present paper, it is assumed that the

fraction of active grains is a function of the volumetric concentration of the bonding material on the grinding wheel since this parameter greatly affects the elasticity of the grinding wheel. Since a grinding wheel is composed of grains, bonding material and air (as internal pores), as can be seen in Figure 4, the volumetric concentration of bonding (V_b) can be estimated from the following equation:

$$V_b = 1 - (V_g + V_p) \tag{10}$$

The volumetric concentration of grains (V_g) can be estimated from equation (9), whereas for the volumetric concentration of the pores (V_p) is a function of the "hardness" number of the grinding wheel, the following equation can be used [16].

$$V_p = \frac{1}{100}\left(45 + \frac{S - 2n}{1.5}\right) \tag{11}$$

Where n is an integer (n=1, 2, 3, 4,…) corresponding to the hardness letter (E, F, G, H, …), respectively. The above equation is valid for grinding wheels having $V_g \leq 60$ %.

For extracting the relationship between the fraction of the active grains and the volumetric concentration, the experimental data stated in [17] and [18] were used. Based on a reference fraction of active grains and the experimental dependence of the number of active grains on the volumetric concentration of bonding material V_b (Figure 3) a normalized factor was introduced.

$$\left(\text{normalized factor}\right) = 20.535 \cdot V_b - 0.217 \tag{12}$$

The fraction active grains can therefore be determined by the following equation:

$$\Phi_a = \Phi_{ref} \times \left(\text{normalized factor}\right) \tag{13}$$

For the definition of the reference fraction the results of Hou and Komanduri [18] have been used. Based on the statistical distribution of abrasive grains to the surface of a grinding wheel and the loading conditions, they have shown that although the number of grains passing through the grinding zone may be a million or more per second, the actual contacting grains are only a small fraction of those (~3 – 4%) and the actual cutting grains even less (~0.15%). This result was obtained for a conventional alumina wheel A46H8V, and thus, the proposed model for estimating the fraction of grains that are active was calibrated for bonding material H, and fraction 3.8 %. For assessing this reference value, in the same paper, in the case of a high material removal rate grinding process, the fraction of the active grains was estimated to be 18% (for grinding A24R6B). The proposed model, for such wheel specifications, estimates the fraction to be 19.5 %.

2.1.3 Average wear flat area

The average wear flat area is considered to be equal to that of a circle having diameter l_{wf} equal to the two-thirds of the average grain diameter:

$$A_g = \tfrac{1}{4}\pi l_{wf}^2 = \frac{\pi d_g^2}{9} \tag{14}$$

Combining equations (2-9) result in the tangential grinding forces due to the grits sliding on the workpiece.

2.1.4 Sliding forces estimation

Based on equation (3), the sliding component of the grinding forces can be estimated using the following closed equation:

$$F_{t,sl} = \frac{3}{100 \times 15.2^2} \mu \cdot \Phi_a \cdot b \cdot l_{wf}^2 \cdot M^2 (32 - S) \sqrt{d_e \cdot a_e} \left[k_1 \frac{4u_w}{d_e \cdot u_s} + k_2 \right] \quad (15)$$

2.2 Cutting forces

The cutting forces can be determined from the specific energy which is defined as the energy expended per unit volume of material removed. The specific energy is given by equation [19]:

$$u_c = \frac{F_{t,c} \cdot u_s}{b \cdot a_e \cdot u_w} \quad (16)$$

where u_c is the specific cutting energy and $F_{t,c}$ is the sum of chip formation and plowing forces.

The cutting energy is the sum of the chip-formation and the plowing energy. It has been shown [16] that the cutting energy asymptotically approaches the chip formation energy as the metal removal rate is increased. Furthermore, it has been proven experimentally that the chip formation energy has a constant value that does not depend on the process parameters, the grinding wheel specifications or the workpiece material. Almost all the relevant studies have indicated an indicative value of specific cutting energy being equal to 13.8 J/mm^3.

Based on the experimental results presented in [16], the following equation can be drawn:

$$u_c = u_{ch} + u_{pl} = u_{ch} + \frac{28.1}{u_w a_e} \quad (17)$$

From equations (10) and (11), the cutting forces can be estimated using the following closed format equation:

$$F_{t,c} = F_{t,ch} + F_{t,pl} = b \cdot a_e \left(\frac{u_s}{u_w} \right)^{-1} \left[u_{ch} + \frac{28.1}{u_w a_e} \right] \quad (18)$$

3 THEORETICAL RESULTS

The model was solved for assessing the effect that process parameters (depth of cut and workpiece speed) and the grinding wheel characteristics (structure, hardness and grain size) have on the grinding forces. The workpiece material considered in the present study, is a typical bearing steel 100 Cr 6. Furthermore, the contribution of the cutting forces to the total forces exerted during grind hardening is discussed. In Table 1, the values of the various coefficients used in the analysis, are presented.

3.1 Cutting forces

The analysis revealed that the grinding wheel characteristics affect the cutting forces exerted for chip formation and plowing. It was found that cutting forces account typically for less than 3% of the total forces. The model predicts that the cutting forces are increased with the depth of cut, whilst the workpiece speed has a negligible effect on them. Furthermore, the utilization of grinding wheels with finer grits – high grain size number – increases the cutting forces. Additionally, harder grinding wheels increase slightly the cutting forces (Figure 5). The structure of the grinding wheel was found to have insignificant effect on the cutting forces.

3.2 Process parameters and grinding wheel effect

The theoretical results showed that the depth of cut has a significant effect on the process forces, whereas the increase of the workpiece speed results in slightly higher process forces (Figure 6).

The hardness of the grinding wheel affects significantly the grinding forces (Figure 6). Utilization of softer wheels results in reduced process forces since grain and bonding fracture occurs more easily and consequently fewer grains interact with the grinding wheel. Using one grade softer grinding wheel in the same process parameters, results in reduced process forces in an average of 10 – 15 %.

The structure number of a grinding wheel represents its porosity. Figure 7 shows that the model predicts increased process forces for “dense” grinding wheels. This is justified by the fact that when using closed structured (denser) wheels, more grains are involved in the process and thus, the actual area of contact in is bigger. Using one grade denser grinding wheel in the same process parameters, results in increased process forces in an average of 5 – 8 %.

The grain size has the smallest effect on the process forces. Utilization of grinding wheels with finer grits results in slightly higher process forces since more grains are involved in the process, and therefore more chips are formed, whilst the cutting forces are increased. The sliding forces, on the other hand, do not depend on the grit size. However, taking into account that the sliding forces are one order of magnitude larger, the overall forces are only slightly increased (Figure 8). Using a

grinding wheel with finer grits by one grade, in the same process parameters, results in increasing the process forces on average by less than 2 %.

4 EXPERIMENTATION

4.1 Experimental setup

For the experimental verification of the model, a number of experiments were designed. Surface up grind-hardening tests were performed on 100 Cr 6 specimens (having rectangular geometry 150 x 80 x 10 mm) with 9 different grinding wheels (having 400mm diameter and 15 mm width). The experimental setup is presented in Table 2, the grinding wheels' specifications that were used are listed in Table 3 and the chemical composition of the workpiece material is presented in table 4. During all the experiments, the process forces were measured by means of a piezo-electronic load cell (Kistler Typ 9067) placed directly between the workpiece spindle and the centre carrying the workpiece.

4.2 Process parameters and grinding wheel effect

Figures 9, 10 and 11 show the comparison between the experimentally measured tangential forces and the theoretical predictions. As it can be seen the theoretical results present the same trends with those of the experiments

The process forces increase as the depth of cut does too and when using grinding wheels presenting greater hardness (Figure 9). The theoretical model could predict with fine accuracy the forces exerted with the use of medium to hard grinding wheels (average deviation from experimental measurements 4%). For softer grinding

wheels, the theoretical model slightly underestimated the exerted forces (8% deviation).

The experimental results showed that by increasing the workpiece speed, the process forces increased as the theoretical model had predicted. The average deviation between the theoretical predictions and the experimental results for changing the workpiece speed varies from 5 to 12%, depending on the grinding wheel structure grade (Figure 10).

Finally, the dependence of the grinding forces on the utilization of grinding wheels with different grit sizes is negligible and lies within the accuracy of the measuring cell used. A comparison with the theoretical predictions showed that the average deviation is in the range of 5 – 9%.

These aforementioned deviations may be attributed to the assumptions made for the simplification of the model and the fact that the forces exerted on the workpiece and the grinding wheel by the coolant fluid are assumed minor.

4.3 Forces Ratio

Cai et al. [20] proved that when no chip forming occurs, the force ratio is identical to the friction coefficient between the grinding wheel and the workpiece. As it was shown in the theoretical results, the force exerted due to chip forming and plowing was negligible (less than 3% of the total forces) in comparison to the sliding force, therefore, the force ratio can be used for assessing the friction coefficient value assumed in the theoretical analysis.

Figures 12 and 13 show the relationship among the force ratio, the depth of cut and the workpiece speed. The dashed line represents the theoretical friction coefficient value used in the analysis. As it can be seen, for small depth of cut values, the experimental results are well represented, however, for larger depth of cut values, the forces ratio presented a greater dispersion. The trend line of the experimental results though, shows good agreement with the theoretical value.

The experiments show a clearer dependence of the forces ratio on the workpiece speed. Therefore, the assumption of a constant friction coefficient is not so realistic, and may be considered as one of the reasons for the greater deviation shown between the experimentally measured forces and the theoretically predicted ones when changing the workpiece speed.

The friction coefficient value used for the theoretical calculations was estimated from literature [18] and can be estimated only experimentally. Its dependence on the workpiece material has not been investigated and it is something to be considered in future studies since in the present one only one workpiece material was considered.

5 CONCLUSIONS

The present study focused on the investigation of the effect the process parameters and grinding wheel characteristics have on the process forces exerted during the grind-hardening process. The developed model takes into consideration the structure, the hardness and the grain size of the grinding wheel.

The process forces are exerted for the sliding of the grits on the workpiece, the chip formation and the plowing of the wokrpiece material. The analysis showed that the sliding forces account for the 97 – 99% of the total forces.

The process parameters affect the process forces, by increasing the depth of cut or the workpiece speed the grinding forces are increased. Furthermore, the process forces are increased when using grinding wheels with harder grade, denser structure or finer grits. The experimental results verified these trends and the theoretical model showed a maximum deviation of 12% from the experimental results. This deviation can be attributed to the assumption of constant friction coefficient and the neglecting of coolant fluid forces.

6 REFERENCES

1 Brinksmeier E, Brockhoff T (1996): Utilisation of Grinding Heat as a New Heat Treatment Process. Annals of the CIRP 45(1):283-286

2 Brockhoff T (1999) Grind-hardening: A comprehensive View. Annals of the CIRP 48(1):255-260

3 Brinksmeier E, Minke E, Wilke T (2005) Investigations on surface layer impact and grinding wheel performance for industrial Grind-Hardening Applications. Production Engineering XII(1):35

4 Chryssolouris G, Tsirbas K, Salonitis G (2005) An analytical, numerical and experimental approach to grind hardening. SME Journal of Manufacturing Processes 7(1):1-9

5 Salonitis K, Chryssolouris G (2007) Cooling application in Grind-Hardening Operations. International Journal of Advanced Manufacturing Technology 33:285

6 Salonitis K, Chryssolouris G (2007) Thermal analysis of Grind-Hardening process. International Journal of Manufacturing Technology and Management, 12:72

7 Salonitis K, Chondros T, Chryssolouris G (2008) Grinding wheel effect in the grind-hardening process. International Journal of Advanced Manufacturing Technology 38:48

8 Chang HC, Wang JJ (2008) A New Model for Grinding Force Prediction and Analysis. International Journal of Machine Tools & Manufacture 48:1335-1344

9 Durgumahanti PU, Singh V, Rao P (2010) A New Model for Grinding Force Prediction and Analysis. International Journal of Machine Tools & Manufacture 50/3:231-240

10 Werner G (1978) Influence of work material on grinding forces. Annals of CIRP 27:243-248.

11 Kumar Mishra V, Salonitis K (2013) Empirical estimation of grinding specific forces and energy based on a modified Werner grinding model. Procedia CIRP 8: 287-292

12 Srihari G, Lal GK (1994) Mechanics of vertical surface grinding. Journal of Materials Processing Technology 44:14-28

13 Chen X, Rowe WB (1996) Analysis and simulation of the grinding process. Part II: Mechanics of grinding. International Journal of Machine Tools and Manufacture 36**:**883-896

14 Torrance AA, Badger JA (2000) The relation between the traverse dressing of vitrified grinding wheels and their performance. International Journal of Machine Tools and Manufacture, 40:1787-1811

15 Badger JA, Torrance AA (2000) A comparison of two models to predict grinding forces from wheel surface topography. International Journal of Machine Tools and Manufacture, 40:1099-1120

16 Malkin S (1989) Grinding Technology: Theory and Applications of Machining with Abrasives, Ellis Horwood, Chichester.

17 Malkin S, Cook NH (1971) The wear of grinding wheels. Part 1. Attritious wear. ASME Journal of Engineering for Industry 93:1120-1128

18 Hou ZB, Komanduri R (2003) On the mechanics of the grinding process – Part I. Stochastic nature of the grinding process, International Journal of Machine Tools and Manufacture 43: 1579-1593

19 Malkin S, Joseph N (1975) Minimum energy in abrasive processes. Wear 32:15-23

20 Cai GC, Feng BF, Jin T, Gong YD (2002) Study on the friction coefficient in grinding. Journal of Materials Processing Technology 129: 25-29

The International Journal of Advanced Manufacturing Technology
January 2014, Volume 70, Issue 1-4, pp 523-530

Table 1. Constants used in equations

Factor	**Value**	**Source**
Friction Coef. μ	0.38	[16]
Emp. Factors	$k_1 = 2.58x10^6$ N/mm $k_2 = 35$ N/mm^2	[4, 16] [4, 16]
Spec. chip energy	$u_{chip} = 13.8$ J/mm^3	[16]
Act. grains ref. fr.	$\Phi_{ref} = 3.8$ %	[18]

Table 2. Experimental setup

Process Parameter	**Value**
Cutting Speed	$U_c = 35$ m/sec
Feed Speed	$U_w = 0.3; 0.6; 0.9$ m/min
Depth of Cut	$a_e = 0.2; 0.3; 0.5$ mm
Coolant characteristics	
Coolant type	Mineral Oil
Pressure	8.5 bar
Flow	2.6 l/min.mm
Nozzle distance	2 mm
Direction	Tangential

Table 3. Grinding Wheels specifications

Grinding Wheel	**Grain size**	**Structure**	**Hardness**
A 60 L7 V	*M* = 60	*S* = 7	L
A 90 L7 V	*M* = 90	*S* = 7	L
A 120 L7 V	*M* = 120	*S* = 7	L
A 60 L5 V	*M* = 60	*S* = 5	L
A 60 L8 V	*M* = 60	*S* = 8	L
A 60 J7 V	*M* = 60	*S* = 7	J
A 60 K7 V	*M* = 60	*S* = 7	K
A 60 M7 V	*M* = 60	*S* = 7	M
A 60 N7 V	*M* = 60	*S* = 7	N

Table 4. Chemical Composition of 100Cr6

Carbon C	Chromium Cr	Iron Fe	Manganese Mn	Phosphorous Ph	Sulfur S	Silicon Si
0.98 – 1.1	1.45	97	0.35	0.025 max	0.025 max	0.23

The International Journal of Advanced Manufacturing Technology
January 2014, Volume 70, Issue 1-4, pp 523-530

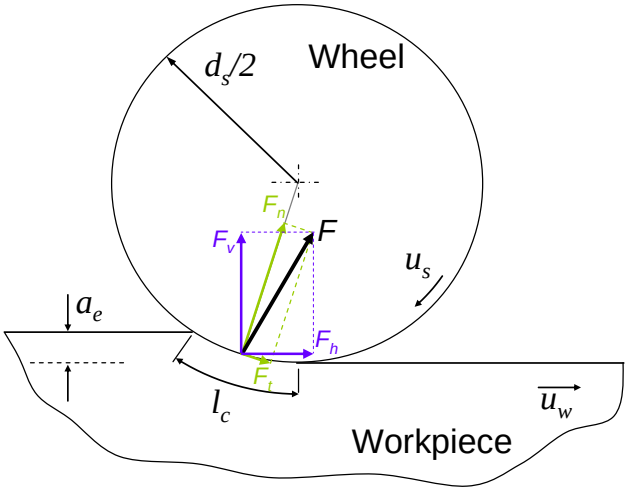

Figure 1: Relationship between grinding force components

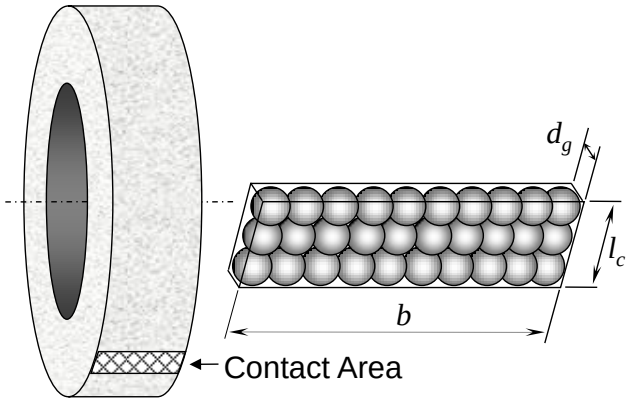

Figure 2: Finite volume for the estimation of the number of the active grains

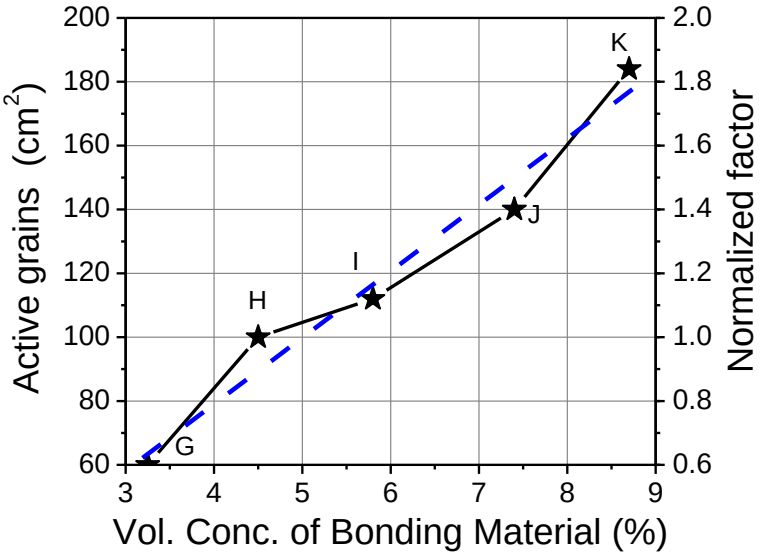

Figure 3: Variation of the number of active grains per unit area with the volumetric concentration of bonding material [11]

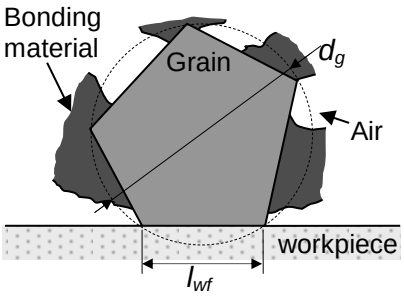

Figure 4. Grain – material interaction

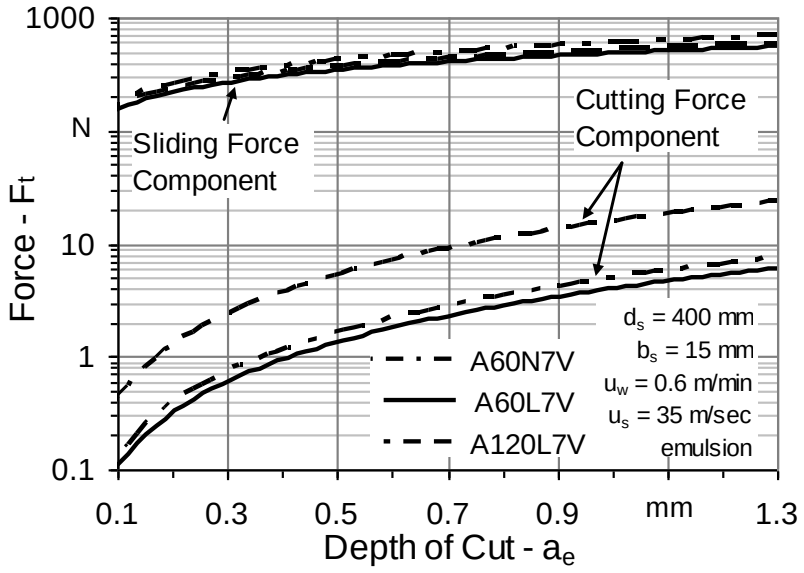

Figure 5. Sliding and cutting forces versus depth of cut

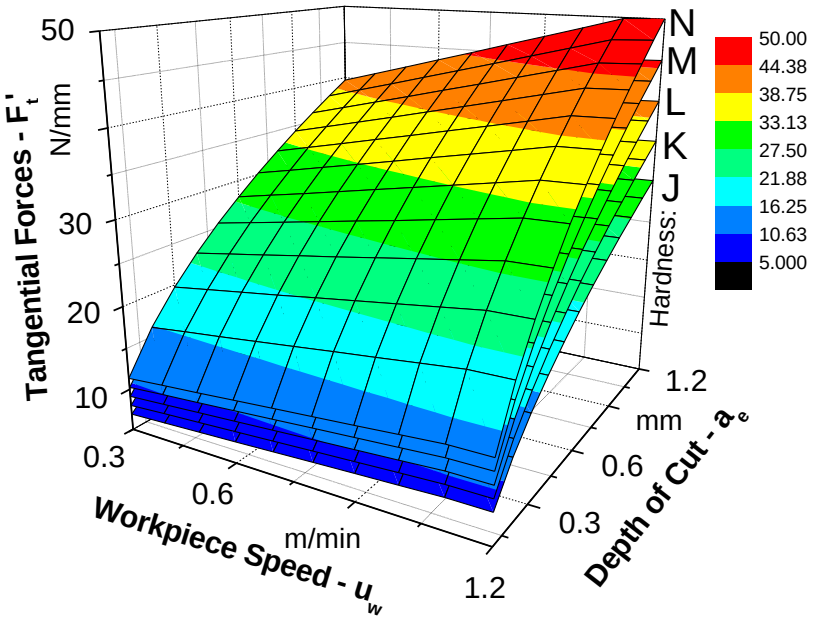

Figure 6. Specific tangential forces as a function of the workpiece speed, the depth of cut and the grinding wheel hardness (Grit size M = 60, Structure S = 7)

The International Journal of Advanced Manufacturing Technology
January 2014, Volume 70, Issue 1-4, pp 523-530

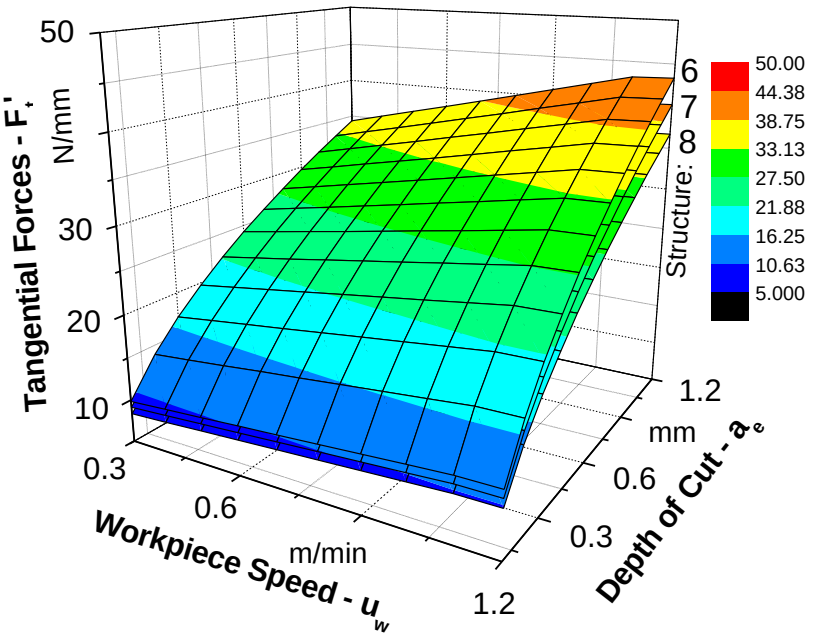

Figure 7. Specific tangential forces as a function of the workpiece speed, the depth of cut and the grinding wheel structure (Grit size M = 60, Hardness L)

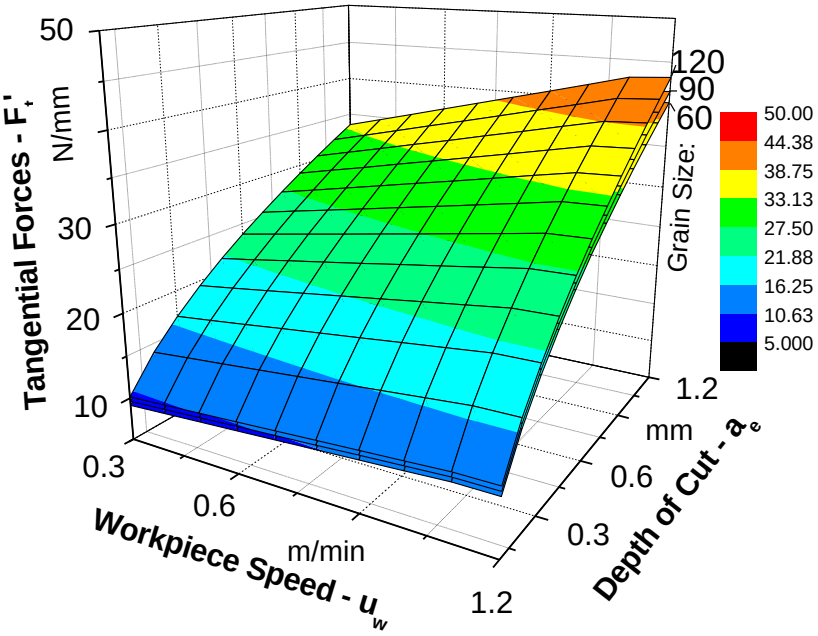

Figure 8. Specific tangential forces as a function of the workpiece speed, the depth of cut and the grinding wheel grain size (Structure S = 7, Hardness L)

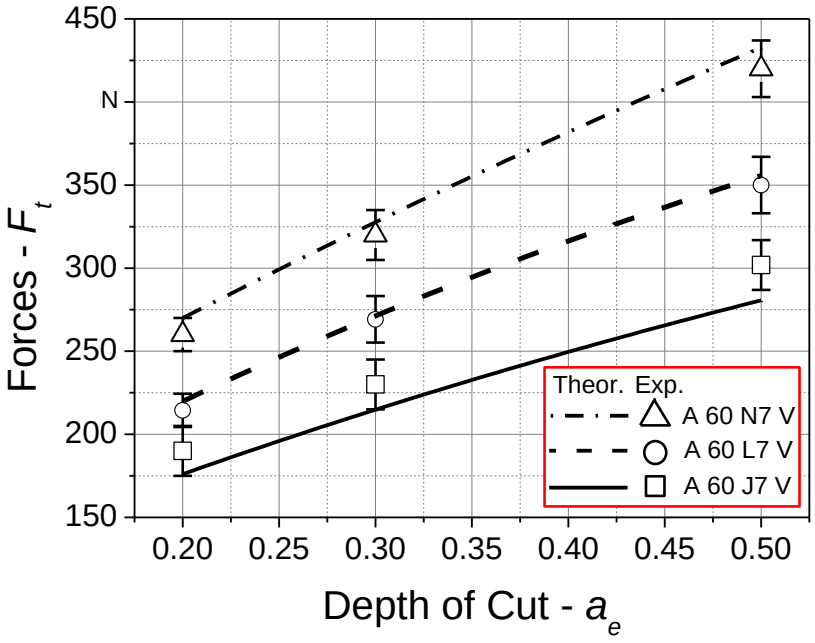

Figure 9. Comparison between experimental measurements and theoretical predictions for grinding wheels with different hardness

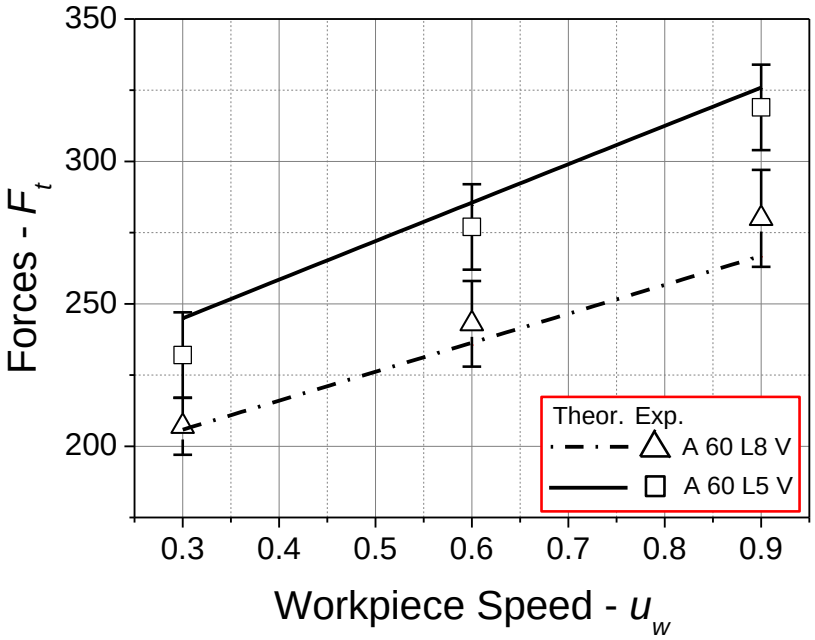

Figure10. Comparison between experimental measurements and theoretical predictions for grinding wheels with different structure grades

The International Journal of Advanced Manufacturing Technology
January 2014, Volume 70, Issue 1-4, pp 523-530

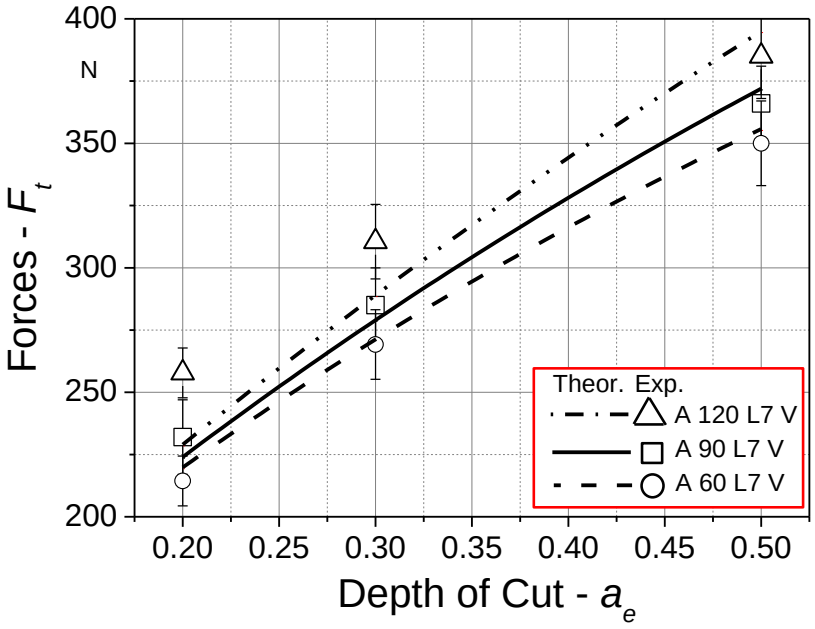

Figure 11. Comparison between experimental measurements and theoretical predictions for grinding wheels with different grit sizes

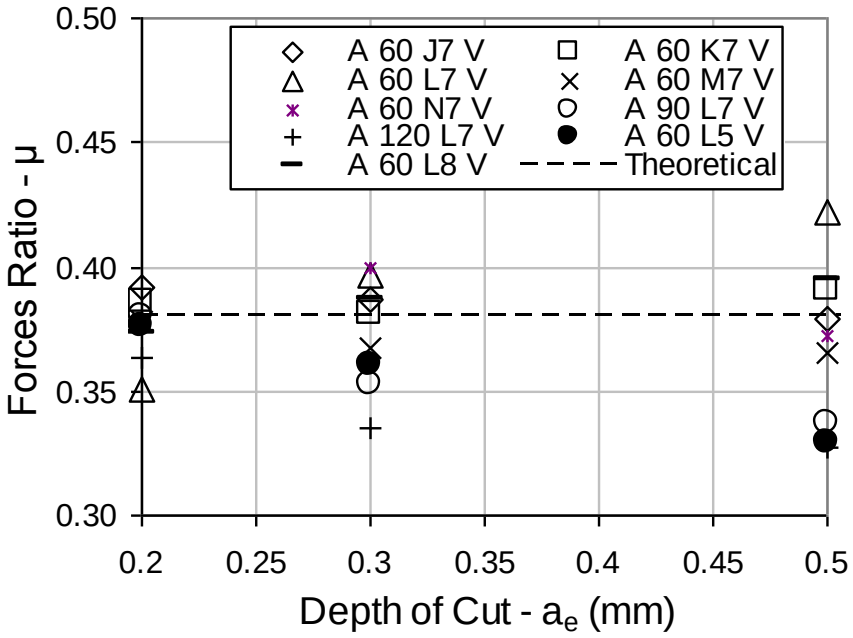

Figure 12. Relationship between grinding force ratio and depth of cut

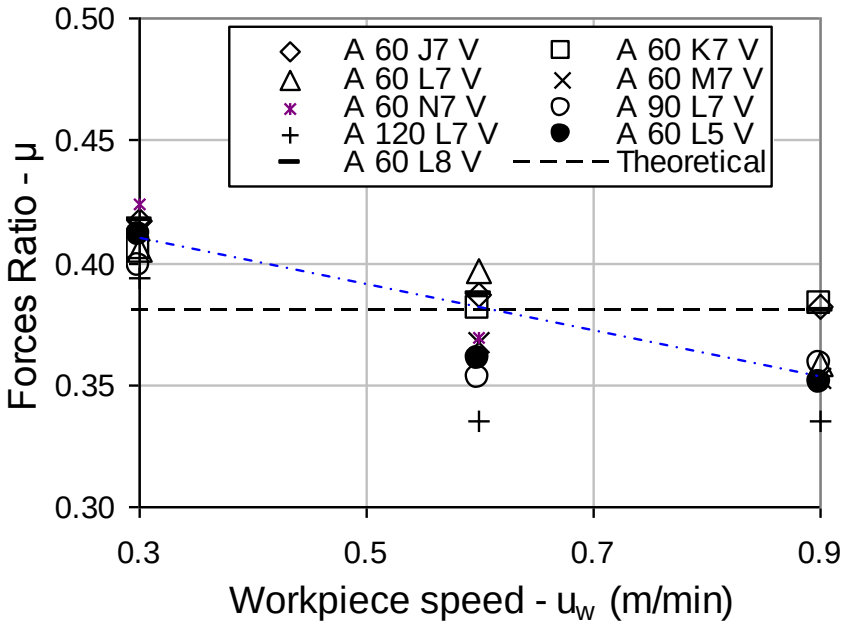

Figure 13. Relationship between grinding force ratio and workpiece speed